Article No. jmbi.1999.2807 available online at http://www.idealibrary.com on IDEAL® J. Mol. Biol. (1999) 289, 981–990

JMB

The Structure of Adrenodoxin Reductase of Mitochondrial *P*450 Systems: Electron Transfer for Steroid Biosynthesis

Gabriele A. Ziegler[1], Clemens Vonrhein[1], Israel Hanukoglu[2] and Georg E. Schulz[1]*

[1]*Institut für Organische Chemie und Biochemie, Albert-Ludwigs-Universität Albertstrasse 21 D-79104 Freiburg im Breisgau Germany*

[2]*E. Katzir Biotechnology Program, Research InstituteCollege of Judea and Samaria Ariel 44837, Israel*

**Corresponding author*

Adrenodoxin reductase is a monomeric 51 kDa flavoenzyme that is involved in the biosynthesis of all steroid hormones. The structure of the native bovine enzyme was determined at 2.8 Å resolution, and the structure of the respective recombinant enzyme at 1.7 Å resolution. Adrenodoxin reductase receives a two-electron package from NADPH and converts it to two single electrons that are transferred *via* adrenodoxin to all mitochondrial cytochromes *P*450. The structure suggests how the observed flavin semiquinone is stabilized. A striking feature is the asymmetric charge distribution, which most likely controls the approach of the electron carrier adrenodoxin. A model for the interaction is proposed. Adrenodoxin reductase shows clear sequence homology to half a dozen proteins identified in genome analysis projects, but neither sequence nor structural homology to established, functionally related electron transferases. Yet, the structure revealed a relationship to the disulfide oxidoreductases, permitting the assignment of the NADP-binding site.

Keywords: crystal structure; disulfide oxidoreductase; electron transferase; flavoenzyme; MAD analysis

Introduction

Adrenodoxin reductase (AdR, NADPH:adrenal ferredoxin oxidoreductase, EC 1.18.1.2) is an FAD-containing enzyme that represents the first component in the mitochondrial cytochrome *P*450 electron transfer systems (Omura *et al*., 1966; Lambeth *et al*., 1982; Hanukoglu, 1992). These systems catalyze hydroxylations converting cholesterol to pregnenolone and then to all steroid hormones as well as hydroxylations in the biosynthesis of bile acids and vitamin D (Bernhardt, 1996). AdR receives electrons from NADPH and transfers them *via* the [2Fe-2S]-ferredoxin-type carrier adrenodoxin (Müller *et al*., 1998) to at least six different cytochromes *P*450 (Hanukoglu, 1992).

In humans there is only one AdR, which is encoded by a nuclear gene and expressed in all human tissues examined. AdR is most abundant in the steroid-producing cells of the adrenal cortex, the ovary and the testis (Hanukoglu, 1992). All proteins of the *P*450 system are located at the matrix side of the inner mitochondrial membrane. AdR and adrenodoxin are easily solubilized proteins, whereas the cytochromes *P*450 are hydrophobic (Hanukoglu, 1992; Bernhardt, 1996). Immunocytochemical studies show, however, that both AdR and adrenodoxin are associated with the mitochondrial membrane, most likely by ionic interactions (Hanukoglu, 1992; Ishimura & Fujita, 1997).

Functionally, AdR has a stabilized semiquinone state (Kobayashi *et al*., 1995) and belongs to a large group of electron transferases that interchange two-electron packages, which are received from or transmitted to NAD(P)H, against single electrons (Massey, 1995). This group includes putidaredoxin reductase (Aoki *et al*., 1998) and NADPH-cytochrome *P*450 reductase (Wang *et al*., 1997) supplying bacterial and microsomal *P*450 systems (Bernhardt, 1996), respectively, as well as the family of the plant-type ferredoxin-NADP$^+$ reductases (Karplus *et al*., 1991). No sequence hom-

Abbreviations used: AdR, adrenodoxin reductase; GR, glutathione reductase; MAD, multiwavelength anomalous dispersion; TrR, thioredoxin reductase; rmsd, root-mean-square deviation; MMA, methylmercury acetate.

E-mail address of the corresponding author: schulz@bio.chemie.uni-freiburg.de

0022-2836/99/240981–10 $30.00/0

ology with these functionally related transferases could be detected. However, a relationship with disulfide oxidoreductases like glutathione reductase had been suggested based on a common sequence fingerprint for NADP-binding (Hanukoglu & Gutfinger, 1989). There is a growing number of proteins identified by genome analyses that are closely related to AdR. Presently, we find seven genes from *Arabidopsis*, yeast and mycobacteria with amino acid sequence identities in the range of 35 % to 40 % in the data banks, constituting an AdR family. Within mammalian AdR the identities are above 85 %.

Several crystal species of AdR (Hiwatashi *et al*., 1976; Nonaka *et al*., 1985; Kuban *et al*., 1993) as well as crystals of a cross-linked complex between AdR and adrenodoxin (Lapko *et al*., 1997) have been reported, yet the AdR structure remained unknown. Here we present this structure, discuss the electron transfer mechanism, and use the relationship with the disulfide oxidoreductases to predict the NADP-binding site. Based on the known structures of adrenodoxin (Müller *et al*., 1998) and its homologue putidaredoxin (Pochapsky *et al*., 1994), we propose a geometry for the interaction of AdR with adrenodoxin.

Results and Discussion

Structure determination

AdR was initially isolated from bovine adrenals and crystallized (Vonrhein *et al*., 1999), but there were not enough suitable crystals for solving the structure. Therefore, the corresponding cDNA was overexpressed in *Escherichia coli* and the recombinant AdR purified to homogeneity (Vonrhein *et al*., 1999). Using the hanging drop vapor diffusion method, three interrelated crystal forms A, A′ and A″ were obtained. The structure was solved in crystal form A″ using a combination of multiwavelength anomalous dispersion (MAD) and isomorphous replacement with a mercury heavy-atom derivative (Table 1).

The resulting electron density map was readily interpretable. The model was built and refined at 2.4 Å resolution. Subsequently, it was transferred to crystal form A′ and refined at 1.7 Å resolution. This model is reported here. The model was then further transferred to crystal form A containing the native enzyme isolated from adrenals and refined at 2.8 Å resolution (Table 2).

Chain fold topology

The enzyme consists of two distinct domains (Figure 1), the chain topologies of which are sketched in Figure 2. The topologies resemble each other; both consist of central parallel β-sheets surrounded by α-helices, the second domain contains an additional three-stranded antiparallel β-sheet. The first domain binds FAD in the usual arrangement across the C-terminal ends of the parallel β-strands at a Rossmann fold (Schulz, 1992). The second domain is inserted between strands β4 and β18 of the FAD-binding domain, which corresponds to a characteristic feature of the disulfide oxidoreductases like glutathione reductase (GR;

Table 1. Data collection and phasing statistics

Data set [a]	A native	A′ recombinant	A″ recombinant	MMA	λ1 edge	λ2 peak	λ3 remote
Wavelength (Å)	0.93	0.91	1.54	0.9057	1.0080	1.0046	0.9918
X-ray source [b]	X11	X11	Cu Kα	X11	X31	X31	X31
Resolution (Å)	32-2.8	34-1.7	29-2.4	53-2.3	41-2.5	40-2.6	40-2.5
Unique reflections	50,561	56,738	17,479	25,010	19,580	17,412	14,245
Redundancy	4.0	4.7	2.4	4.1	3.6	3.6	2.5
Completeness (%)[c]	87 (62)	93 (76)	74 (37)	99 (95)	100 (100)	100 (97)	73 (40)
R_{sym} (%)[c,d]	20.6 (37)	4.9 (24)	4.8 (13)	4.3 (15)	5.9 (21)	5.2 (20)	5.5 (21)
I/σ_I[c]	2.1 (1.8)	10.8 (3.1)	11.0 (4.9)	9.0 (4.9)	8.2 (3.5)	8.5 (3.8)	11.4 (3.1)
Phasing power[e]							
Isomorphous[f]			1.6 (1.2)	2.5 (1.2)	1.6 (1.0)	1.2 (0.6)	-
Anomalous			-	2.6	1.9	2.6	2.4
Scattering factor f' (e^-)[g]			-	-	−17.3	−12.1	−10.6
Scattering factor f'' (e^-)[g]			-	-	3.9	10.0	8.8

[a] All crystals belong to space group $P2_1$. The unit cell parameters are: form A, $a = 85.7$ Å, $b = 63.1$ Å, $c = 219.0$ Å, $\beta = 94.4°$; form A′, $a = 60.8$ Å, $b = 62.5$ Å, $c = 78.4$ Å, $\beta = 106.8°$; form A″, $a = 57.8$ Å, $b = 62.0$ Å, $c = 83.0$ Å, $\beta = 107.1°$; derivative MMA, $a = 57.6$ Å, $b = 62.0$ Å, $c = 82.1$ Å, $\beta = 106.5°$; MAD data sets λ1, λ2 and λ3, $a = 57.7$ Å, $b = 62.0$ Å, $c = 83.0$ Å, $\beta = 107.0°$. Crystal form A is related to A′ and A″. The unit cell of form A is four times larger than those of the others (Vonrhein *et al*., 1999). The mercury derivative was produced by soaking with 0.05 mM methylmercury acetate in buffer C with 12 % (w/v) PEG-8000 and 10 % (v/v) glycerol for about ten hours at 20 °C.

[b] Beam lines X11 and X31 are at the EMBL-outstation (Hamburg). All data were collected at 100 K, except for data set A that was collected at 300 K.

[c] The last shell values are given in parentheses.

[d] $R_{sym} = \Sigma_{hkl,i}|I_{hkl,i} - \langle I_{hkl}\rangle|/\Sigma_{hkl,i}I_{hkl,i}$.

[e] Using program SHARP. The phasing power is the heavy-atom signal divided by the error.

[f] Data for the acentric reflections. The values for the centrics are given in parentheses.

[g] As derived from a fluorescence scan. After refinement the values changed on average by 1.8 e^-.

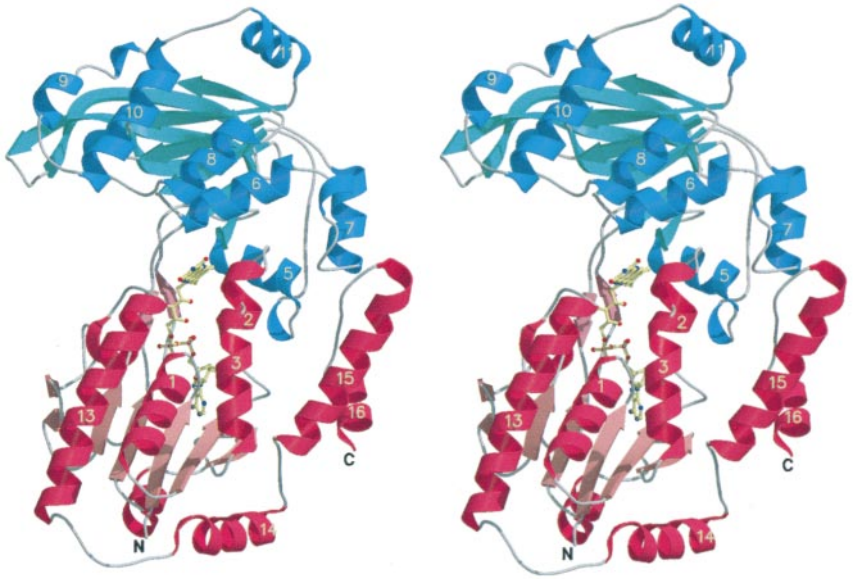

Figure 1. Stereo view of the AdR chain fold. The termini and some α-helices are labeled. The prosthetic group FAD (yellow) and the subdivision into FAD-domain (red) and ''NADP''-domain (blue) are shown.

Schulz *et al*., 1978). The relationship was confirmed by a general search for similar structures in the Protein Data Bank using distance matrix techniques (Holm & Sander, 1993), that retrieved the disulfide oxidoreductase NADH-peroxidase (Stehle *et al*., 1991) as the closest match.

In GR the two domains bind FAD and NADP at corresponding positions of closely similar domain topologies giving rise to the proposal that they originated from a gene duplication (Schulz, 1980). This may also apply for AdR, where however, the relationship is more distant because the FAD-domain of AdR lacks the characteristic antiparallel β-sheet (strands β11, β12 and β13 of the ''NADP''-domain; Figure 2) that occurs in both dinucleotide-binding domains of GR.

Functionally, AdR is a close relative of the plant ferredoxin-$NADP^+$ reductase (Karplus *et al*., 1991), because both enzymes use NADP, FAD and an iron-sulfur single-electron carrier protein. Moreover, the carriers are homologous (Müller *et al*., 1998) and a blue semiquinone is stabilized in both reactions (Kobayashi *et al*., 1995; Massey, 1995). A structural relationship was therefore expected. A comparison with AdR shows clearly, however, that the chain topologies are different, which applies also for the other structurally known electron transferases (Correll *et al*., 1992; Lu *et al*., 1994; Nishida *et al*., 1995; Wang *et al*., 1997; Ingelman *et al*., 1997) all of which have the ferredoxin-$NADP^+$ reductase fold. AdR is therefore an outlier among the single electron transferases that has converged to a similar function during evolution.

FAD-binding site

FAD is very well defined in the electron density map (Figure 3). Its conformation is virtually identical with that of FAD in the disulfide oxidoreductases, FAD superpositions resulted in rms deviations around 0.6 Å. The two negative charges of the phosphate diesters are compensated by the dipole moment of helix α1, and *via* water by Arg124 in helix α5. The ribose is tightly bound to Glu38 at the carboxy-terminal end of strand β2, as commonly observed with dinucleotides (Schulz, 1992).

Table 2. Refinement statistics

Crystal form	A	A′	A″
Resolution range (Å)	20-2.8	18-1.7	29-2.4
Number of protein atoms[a]	14,228	3557	3557
Number of solvent molecules	0	587	91
R-factor (%)[a]	27.9	18.8	20.3
R_{free} (%)[b]	31.2	22.3	26.3
rmsd bond lengths (Å)	0.010	0.013	0.013
rmsd bond angles (°)	2.3	2.3	2.7
Average *B*-factor FAD-domain (Å^2)	18	25	34
Average *B*-factor ''NADP''-domain (Å^2)	31	28	52
rmsd of *B*-factors along bonds (Å^2)	2.5	1.8	1.9
rmsd of *B*-factors along angles (Å^2)	3.8	2.7	2.9

[a] The enzyme consists of 460 amino acid residues and FAD with an M_r of 51,079. The N-terminal residues are not visible.
[b] R-factor $= \Sigma_{hkl}||F_{obs}| - k|F_{calc}||/\Sigma_{hkl}|F_{obs}|$, R_{free} is the R-factor for a set of 5 % randomly chosen reflections that are not included in the refinement.

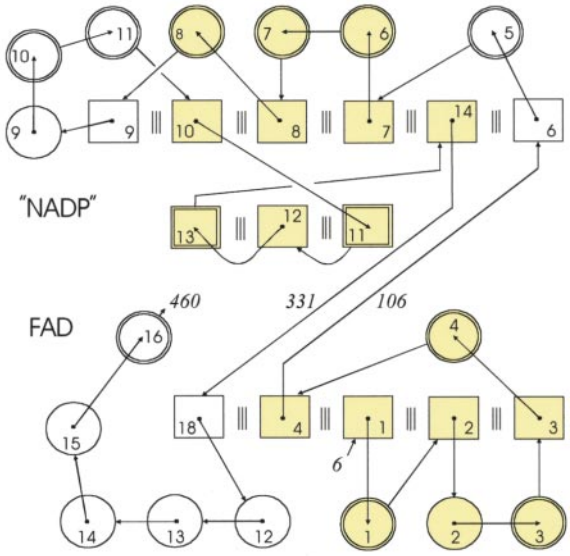

Figure 2. Sketch of the AdR chain fold topology using squares for β-strands and circles for α-helices. Double lines mark reverse directions (view onto the N terminus of the element). Triple vertical lines indicate hydrogen bonding. Four short antiparallel β-strands and five short 3_{10}-helices are omitted for clarity. The two central parts that usually define the binding sites of the dinucleotides are colored. In glutathione reductase the equivalent parts bind FAD and NADP, which prompted us to name the insert ''NADP''-domain.

FAD binds in an elongated conformation with the isoalloxazine portion pointing towards the ''NADP''-domain and the adenine portion buried in the FAD-domain. The *si*-face of the isoalloxazine is covered by the polypeptide chain, whereas the *re*-face is solvent-exposed, similar to the FAD-binding mode in the disulfide oxidoreductases. This contrasts with the FAD-binding geometry of the ferredoxin-$NADP^+$ reductase family, where the *si*-face is solvent-exposed (Karplus *et al.*, 1991; Wang *et al.*, 1997; Ingelman *et al.*, 1997).

The isoalloxazine of AdR, however, is less tightly packed into the polypeptide than in the disulfide oxidoreductases. Its O2 atom is stabilized by a hydrogen bond to Ile376-N (Figure 3), and its O4 and N5 atoms are stabilized through hydrogen bonds to a water molecule that is fixed by the side-chains of His55 and Asp159. With His55 as secondary contact, this water molecule can easily protonate the N5 atom and thus stabilize the intermediate semiquinone as the observed blue neutral radical (Kobayashi *et al.*, 1995).

Structure comparison with thioredoxin reductase

When separating the AdR chain into the FAD and ''NADP''-domains, a general comparison with the Protein Data Bank (Holm & Sander, 1993) results in best fits with the two thioredoxin

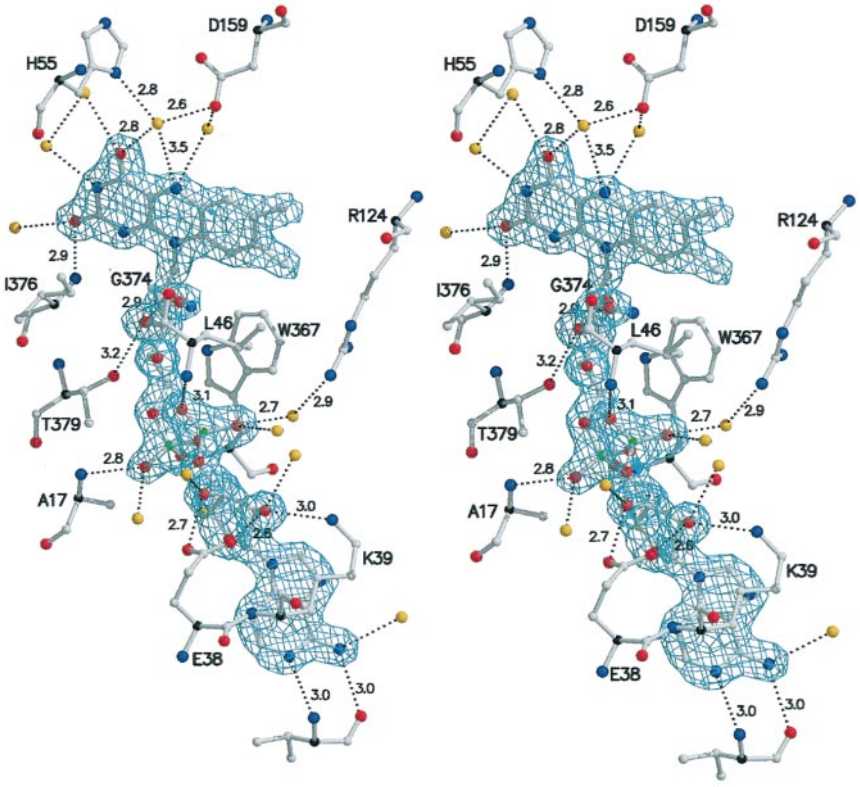

Figure 3. FAD as bound to AdR together with the final ($2mF_o - DF_c$) map contoured at 2.0 σ in crystal form A′ at 1.7 Å resolution. Hydrogen bonds are given with their lengths (dotted lines). The C^α atoms of the polypeptide fragments are in black. The residue at the bottom is V82.

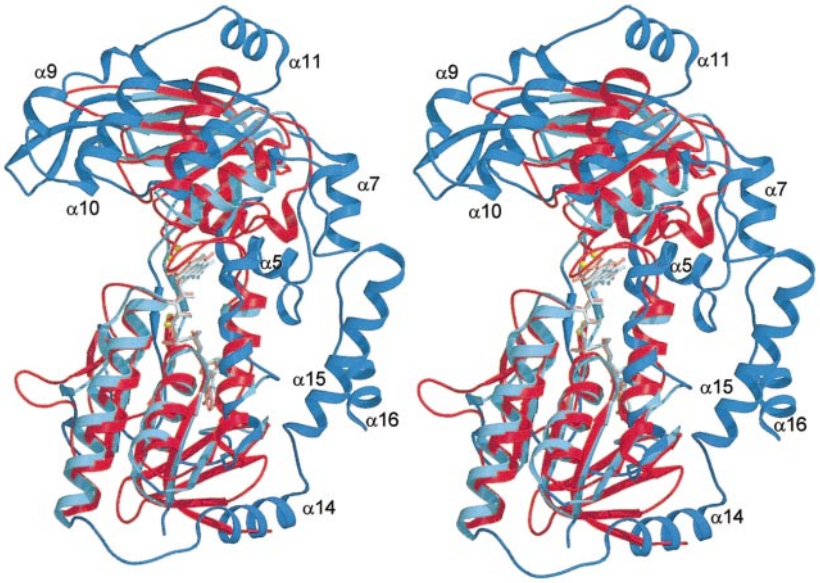

Figure 4. Domain-by-domain superposition of AdR (blue) with thioredoxin reductase from *E. coli* (TrR, red). Because of the rotational deviations of the FAD and NADP-domains, the TrR chain had to be cut twice. The four cuts are marked by yellow balls (near to the isoalloxazine). The FAD of TrR (pink) and the FAD of AdR (blue) superimpose very well. In contrast to the 460 residues of the monomeric AdR, TrR from *E. coli* is a dimer of 316 residue chains. A total of 196 C^{α} atoms (110 of the FAD-domain and 86 of the ''NADP''-domain) in 19 segments could be superimposed using LSQKAB (CCP4, 1994) with a 3 Å cutoff criterion. The sequence identity in the equivalenced segments is 21 %.

reductase (TrR) domains (Waksmann *et al*., 1994; Dai *et al*., 1996; Figure 4). AdR and TrR differ strongly with respect to the domain arrangement; the NADP-domains show a rotational deviation of 66° if the FAD-domains are superimposed. The observed arrangement of TrR, however, has to change during catalysis where the NADP-domain presumably runs through an AdR-like (i.e. GR-like) position (Waksmann *et al*., 1994). The domain-by-domain superposition of TrR and AdR is illustrated in Figure 4. AdR contains three additional α-helices (α14, α15 and α16) at the C terminus and two additional α-helices in the ''NADP''-domain (α5 and α7) that together strengthen the domain interface appreciably. Two further inserted helices in the ''NADP''-domain of AdR (α9, α10) contain the two arginine residues essential for electron transfer (see below).

Putative NADP-binding site

A chain fold comparison (Holm & Sander, 1993) between the complete AdR and the disulfide oxidoreductases yielded flavocytochrome *c* sulfide dehydrogenase (Chen *et al*., 1994) and GR as the second best fits after NADH-peroxidase (Stehle *et al*., 1991**)** as the best. We decided to focus on GR because it uses NADP similar to AdR. A superposition shows that the chain folds fit with respect to the two parallel β-sheets and some surrounding residues in the two domains (Figure 5), indicating that the general construction principle and the domain arrangements are identical.

In the canonical structures, dinucleotides always bind across the carboxy-terminal ends of central parallel β-sheets with the phosphate diesters at the loop between first β-strand and following α-helix (Schulz, 1992). Consequently, not only the central β-sheets of AdR and GR are equivalent but also the dinucleotide binding modes. As shown in Figure 5 this is correct for FAD. Assuming that the superposition applies also for the other dinucleotide, we transferred the NADP ligand of GR to AdR and observed a good fit. The putative NADP-binding site of AdR agrees with the sequence fingerprint (Hanukoglu & Gutfinger, 1989) and with NMR data (Miura & Ishikawa, 1994), and it gives rise to a reasonable interaction geometry between the nicotinamide and isoalloxazine moieties of the ligands (Figure 5). One may speculate that the required interaction between NADP and FAD has conserved the central β-sheets in their relative arrangement during evolution despite the large changes in other parts.

Proposed interactions with adrenodoxin

There is a striking charge segregation on the AdR surface (Figure 6), rendering the cleft between the FAD and the NADP-domains almost completely basic, while the opposite side of the molecule is predominantly acidic. The charges are balanced, because the isoelectric point ranges around 7 as determined by isoelectric focussing. The electric field of AdR most likely steers the approach of adrenodoxin ($M_r = 14{,}222$), which is dipolar itself with negative charges near its iron-sulfur cluster (Müller *et al*., 1998). This agrees with the observed ionic strength effects (Lambeth *et al*., 1979). Moreover, these asymmetries resemble those of the cytochromes *P*450 (Hasemann *et al*., 1995), suggesting that all steroidogenic electron transfers in mitochondria, like many other electron transfers, are mediated by electrostatic interactions (Lambeth *et al*., 1979; Hanukoglu *et al*., 1981; Hasemann *et al*., 1995).

Mutagenesis experiments on AdR revealed that residues Arg240 and Arg244 (bovine numbering, marked in Figure 6) are important for the association with adrenodoxin (Vickery, 1997). These residues are located at a highly basic patch at the edge of the cleft. Corresponding mutagenesis studies

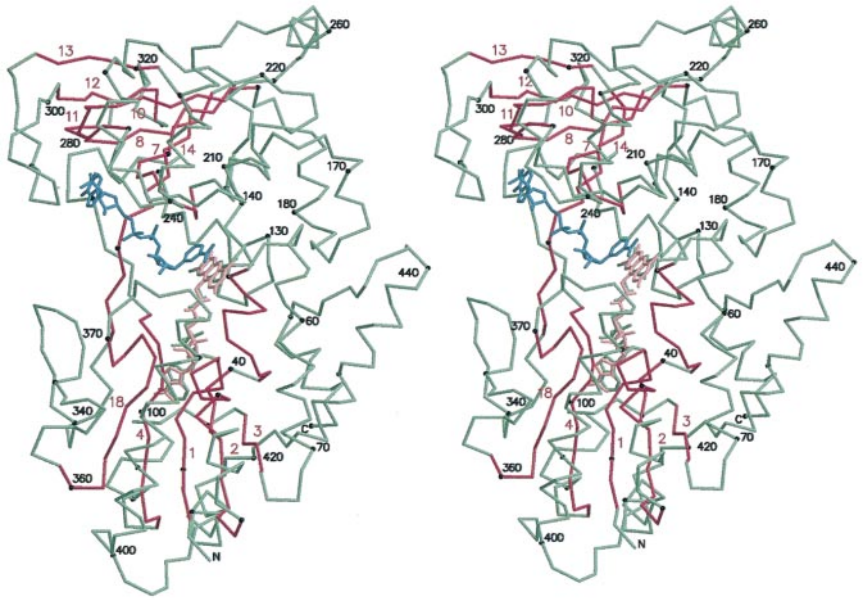

Figure 5. AdR as superimposed with glutathione reductase (GR). For clarity, only the AdR chain fold is depicted and the superimposed segments are marked (red). Every tenth AdR position carries a black dot, some of them are labeled. In total, 126 C^{α} atoms (65 of the FAD and 61 of the ''NADP''-domain) in 12 segments were superimposed (CCP4, 1994) within a 3 Å cutoff criterion. The FAD position in GR (pink) is well conserved in AdR (green). NADP as bound to GR is inserted (blue). Like in GR and other disulfide oxidoreductases it sandwiches to FAD. The putative NADP model does not seriously collide with AdR and also not with adrenodoxin in the modeled complex of Figure 6.

with the carrier showed that residues Asp76 and Asp79 of adrenodoxin are crucial for the interaction, and it has been proposed that these aspartate residues contact the two arginine residues of the reductase (Vickery, 1997). Furthermore, the complex could be cross-linked between Lys66 of adrenodoxin and Glu4 of AdR (Hara & Miyata, 1991). It was also shown that the C terminus of adrenodoxin (20 residues beyond position 108) is rather mobile but important for binding to the reductase (Uhlmann *et al*., 1994). The location of residue 108 can be derived from the structure of C-terminally truncated adrenodoxin (Müller *et al*., 1998). The homologous structure of putidaredoxin (Pochapski *et al*., 1994) shows four additional C-terminal residues. Both positions are indicated in Figure 6, together with a groove of AdR that could well accomodate the C-terminal chain. Based on these structural restraints we manually docked adrenodoxin at the basic cleft of AdR. The resulting electrostatic interactions at the interface were favorable.

Given this fit, the [2Fe-2S] cluster of adrenodoxin is at a distance of 16 Å from the center of the isoalloxazine of AdR, suggesting the electron transfer pathway shown in Figure 7. A similar long-range electron transfer occurs in cytochrome *c* oxidase over a 19 Å distance through 14 covalent and two hydrogen bonds (Gray & Winkler, 1996). Even if we dispense with the above-mentioned docking restraints, the geometries of AdR and adrenodoxin prohibit a reduction of the electron transfer distance below 11 Å in any relative orientation. This distance is much larger than the observed distance in phthalate dioxygenase reductase (Correll *et al*., 1992) that belongs to the ferredoxin $NADP^+$ reductase family and thus to a structurally quite different group of proteins.

Surprisingly, the fit between AdR and adrenodoxin is not disturbed by NADP when bound, as proposed in Figure 5. Moreover, the nicotinamide moiety of bound NADP fills the cavity completely at the *re*-side of the isoalloxazine, which probably contains water in the binary complex. From a structural point of view the electron transfer from AdR to adrenodoxin may therefore occur in the presence of NADPH or $NADP^+$, which is consistent with NMR studies (Miura & Ishikawa, 1994) and had been suggested by Kobayashi *et al*. (1995).

The proposed complex neglects a conceivable induced-fit on adrenodoxin-binding. However, the conformational changes in AdR are most likely small because there are no detectable differences between the three crystal packings. Yet, the *B*-factors of the ''NADP''-domain are higher than those of the FAD-domain (Table 2), indicating some leeway. We therefore expect displacements up to 1 Å upon complex formation. Similar changes have been reported for adrenodoxin when binding to AdR (Miura & Ishikawa, 1994).

Glycosylation

There are contradictory reports on whether AdR is glycosylated or not (Hiwatashi *et al*., 1976; Ichikawa & Hiwatashi, 1982; Suhara *et al*., 1982; Wartburton & Seybert, 1995; Sagara *et al*., 1993). As expected for a mitochondrial matrix protein, the sequence contains no *N*-glycosylation fingerprint. A search for putative *O*-glycosylation sites (Hansen *et al*., 1995) revealed two predicted sites at Thr314 and Thr378 and three further sites with substantial probabilities at Thr254, Thr373 and Thr381. All these residues are at the molecular surface. In a further investigation we solved the structure of crystal form A of the native bovine enzyme (Table 2). Since we used the recombinant, non-glycosylated enzyme of crystal form A′ as the starting model for the refinement, any carbohydrate should appear with positive difference

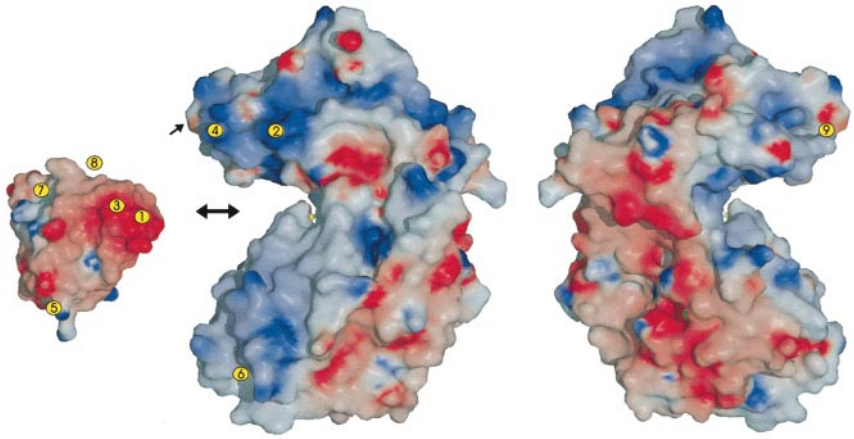

Figure 6. Surface representation of AdR and of an adrenodoxin molecule (Müller *et al.*, 1998) colored according to the electrostatic potential from blue (positive) to red (negative) (Nicholls *et al.*, 1991). The view of AdR at the right-hand-side is rotated by 180° around a vertical axis. The adrenodoxin molecule is oriented according to the following observations: (i) Asp76 (label 1) and Asp79 (label 3) match with Arg244 (label 2) and Arg240 (label 4), respectively; (ii) Lys66 (label 5) can be cross-linked with Glu4 (label 6); (iii) the C-terminal residue of the truncated adrenodoxin structure (label 7) and the C-terminal end of the homologous putidaredoxin structure (Pochapsky *et al.*, 1994) (label 8) point to a groove between α9 and β12 at the surface of AdR (label 9). This groove is a specialty of AdR and could readily accommodate the long, presumably mobile C-terminal chain end of adrenodoxin. In the proposed complex, the electrostatic interactions of the respective surfaces of AdR and adrenodoxin are favorable.

density. A thorough search, in particular at the predicted sites, failed to show any positive peak of appropriate size anywhere in two ($mF_o - DF_c$)-difference maps at 2.8 Å and at 3.5 Å resolution, indicating that, in agreement with earlier data (Wartburton & Seybert, 1995; Sagara *et al.*, 1993), bovine AdR is not glycosylated. It should be mentioned that a carbohydrate at positions 373 or 378 would be incompatible with the adrenodoxin docking model in Figure 6.

Conclusion

Bovine AdR is an electron transferase with a striking asymmetric charge distribution controlling the approach of the asymmetrically charged electron carrier adrenodoxin. AdR is structurally and therefore most likely evolutionary related to the disulfide oxidoreductases and shows no chain fold similarity with the functionally related ferredoxin-$NADP^+$ reductase family. No glycosylation could be detected. Modeling studies indicate that the electrons tunnel over a distance of 16 Å, possibly in the presence of NADP(H).

Materials and Methods

Over-expression, purification and crystallization

The native enzyme was isolated and purified as described (Vonrhein *et al.*, 1999). For producing the recombinant enzyme, *E. coli* strain BL21(DE3) carrying a modified bovine AdR-encoding plasmid was transformed with a plasmid encoding the HSP60-chaperone system. For avoiding inclusion bodies, the temperature was lowered to 20°C after induction. AdR was isolated by ion exchange chromatography followed by an affinity chromatography using 2′-5′-ADP-Sepharose (Vonrhein *et al.*, 1999). All AdR crystals were grown with the hang-

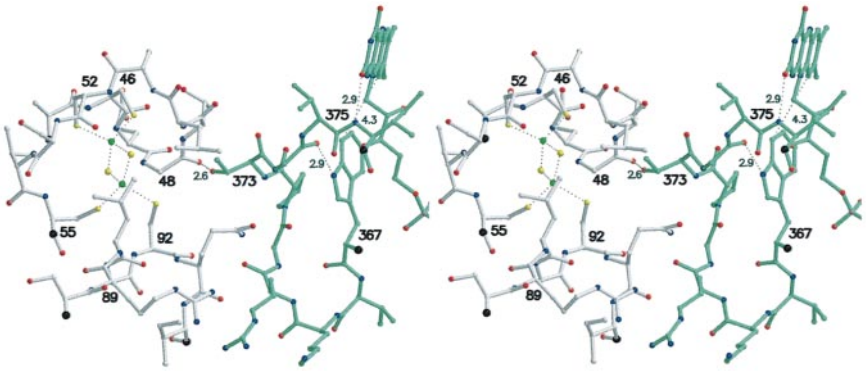

Figure 7. Modeled complex between AdR (green) and adrenodoxin (grey) using the orientations of Figure 6, where the docking is rationalized. The distance between the isoalloxazine and the [2Fe-2S] cluster is 16 Å. The electron transfer is likely to proceed from the benzene moiety of isoalloxazine, *via* Trp367 and the main-chains of AdR and adrenodoxin to the cluster.

ing drop vapor diffusion method. For crystal form A the droplet contained buffer C (50 mM sodium cacodylate (pH 6.5), 100 mM calcium acetate) with 4 mg/ml protein and 8 %(w/v) PEG-8000, whereas the reservoir consisted of 12 %(w/v) PEG-8000 in buffer C. Crystal forms A′ and A′′ grew under the same conditions except that 5 % (v/v) glycerol was added to the droplet (Vonrhein *et al*., 1999).

Crystals appeared after one day at 20 °C and grew within three days to their final sizes of about 150 μm × 150 μm × 1500 μm. All crystal habits were identical. It turned out that there are only small molecular packing differences between the three forms. Form A′ and A″ crystals were transferred stepwise into cryoprotectant (buffer C with 12 %(w/v) PEG-8000 and 20 % (v/v) glycerol) and then mounted in a loop, shock-frozen in a 100 K nitrogen gas stream and kept therein.

Data collection

The data sets A, A′, A″ and MMA were collected using synchrotron radiation (EMBL-Hamburg) or a rotating anode (Rigaku RU200B) as specified in Table 1. They were processed with programs XDS (Kabsch, 1988), MOSFLM (Leslie, 1990) and SCALA (CCP4, 1994). The search for heavy-atom derivatives resulted in only one stable crystal modification (MMA) with axes similar to one of the native data sets, namely to crystal form A″. Since this derivative showed a strong anomalous signal it was used for MAD phasing. The MAD data were collected on beamline X31 at the synchrotron EMBL-Hamburg on an 18 cm-MAR image plate detector. Due to their natural elongated shape, the crystals could readily be oriented with their *b*-axis parallel with the spindle axis, allowing nearly simultaneous recording of Friedel pairs. The edge (λ1 at the inflection point), peak (λ2) and remote (λ3) wavelengths were determined by a fluorescence scan (Table 1). The MAD data were processed with programs MOSFLM (Leslie, 1990) and SCALA (CCP4, 1994), using data set λ3 as the reference. Structure factors were calculated with program TRUNCATE (CCP4, 1994). Data sets A″ and MMA were scaled onto data set λ3 using program SCALEIT (CCP4, 1994).

Phasing

The mercury positions (Table 1) were established with difference-Patterson maps. There were two major sites at Cys74 and Cys322 and less well occupied sites at Cys145 and Cys364. Three of the mercury atoms appeared also in an anomalous Patterson map using the peak wavelength (λ2) data set. The MAD data sets were combined with sets A″ and MMA for heavy-atom refinement and phasing using program SHARP (de la Fortelle & Bricogne, 1997). Assuming one molecule in the asymmetric unit, a solvent content of 52 % was used in solvent-flattening with program SOLOMON (Abrahams & Leslie, 1996). The resulting electron density map was clearly interpretable.

Model building and refinement

A partial initial model which had been obtained in crystal form A, but could not be improved beyond an *R*-factor of about 50 % (unpublished results), was transferred into the solvent-flattened map of the related crystal form A″. The model was corrected and completed using the program O (Jones *et al*., 1991) and refined with program REFMAC (CCP4, 1994) using the bulk solvent correction of X-PLOR (Brünger, 1993). Ordered water molecules were added using ARPP (CCP4, 1994). Subsequently the model was transferred into crystal form A′, and the structure was refined with REFMAC/X-PLOR/ARPP to 1.7 Å resolution.

The resulting model was then transferred to crystal form A and refined at 2.8 Å resolution in order to check for differences between the recombinant and the native enzyme. For this transfer we used the observation that the four AdR molecules in the asymmetric unit of crystal form A were only slightly displaced from an average position corresponding to a four-times smaller unit cell (Vonrhein *et al*., 1999). During refinement, the four AdR molecules were strongly restrained by non-crystallographic symmetry for 438 residues outside crystal contacts. The resulting displacements from the average (small unit cell) position were about 1 Å.

Protein Data Bank accession numbers

The coordinates and structure factors are deposited with the Protein Data Bank, Brookhaven, under accession number 1CJC.

Acknowledgments

We thank the EMBL-team (Hamburg) for helping with synchrotron data collection. We further thank U. Heinemann for providing the adrenodoxin coordinates prior to general release as well as T. Schwede and L. Maveyraud for discussions. This work was supported by the Deutsche Forschungsgemeinschaft under Sfb-388. G.A.Z. and C.V. contributed equally to this work.

References

Abrahams, J. P. & Leslie, A. G. W. (1996). Methods used in the structure determination of bovine mitochondrial F1 ATPasse. *Acta Crystallog. sect. D,* **52**, 30-42.

Aoki, M., Ishimori, K. & Morishima, I. (1998). NMR studies of putidaredoxin: association of putidaredoxin with NADH-putidaredoxin reductase and cytochrome *P*450cam. *Biochim. Biophys. Acta,* **1386**, 168-178.

Bernhardt, R. (1996). Cytochrome *P*450: structure, function and generation of reactive oxygen species. *Rev. Phys. Biochem. Pharmacol.* **127**, 137-221.

Brünger, A. T. (1993). *X-PLOR version 3. 1 a system for X-ray crystallography and NMR,* Yale University Press, New Haven.

Chen, Z. W., Koh, M., Van Driessche, G., Van Beeumen, J. J., Bartsch, R. G., Meyer, T. E., Cusanovich, M. A. & Mathews, F. S. (1994). The structure of flavocytochrome *c* sulfide dehydrogenase from a purple phototrophic bacterium. *Science,* **266**, 430-432.

Collaborative Computational Project Number 4 (1994). The CCP4 suite: programs for protein crystallography. *Acta Crystallog. sect. D,* **50**, 760-763.

Correll, C. C., Batie, C. J., Ballou, D. P. & Ludwig, M. L. (1992). Phthalate dioxygenase reductase: a modular structure for electron transfer from pyridine nucleotides to [2Fe-2S]. *Science,* **258**, 1604-1610.

Dai, S., Saarinen, M., Ramaswany, S., Meyer, Y., Jacquot, J.-P. & Eklund, H. (1996). Crystal structure of *Arabidopsis thaliana* NADPH dependent thiore-

doxin reductase at 2.5 Å resolution. *J. Mol. Biol.* **264**, 1044-1057.

de la Fortelle, E. & Bricogne, G. (1997). Maximum-likelihood heavy-atom parameter refinement for multiple isomorphous replacement and multiwavelength anomalous diffraction methods. *Methods Enzymol.* **276**, 472-493.

Gray, H. B. & Winkler, J. R. (1996). Electron transfer in proteins. *Annu. Rev. Biochem.* **65**, 537-561.

Hansen, J. E., Lund, O., Engelbrecht, J., Bohr, H., Nielson, J. O., Hansen, J.-E. S. & Brunak, S. (1995). Prediction of *O*-glycosylation of mammalian proteins: specificity patterns of UDP-GalNAc:polypeptide *N*-acetylgalactosaminyltransferase. *Biochem. J.* **308**, 801-813.

Hanukoglu, I. (1992). Steroidogenic enzymes: structure, function, and role in regulation of steroid hormone biosynthesis. *J. Steroid Biochem. Mol. Biol.* **43**, 779-804.

Hanukoglu, I. & Gutfinger, T. (1989). cDNA sequence of adrenodoxin reductase. *Eur. J. Biochem.* **180**, 479-484.

Hanukoglu, I., Privalle, C. T. & Jefcoate, C. R. (1981). Mechanisms of ionic activation of adrenal mitochondrial cytochromes P-450scc and P-45011β. *J. Biol. Chem.* **256**, 4329-4335.

Hara, T. & Miyata, T. (1991). Identification of a cross-linked peptide of a covalent complex between adrenodoxin reductase and adrenodoxin. *J. Biochem.* **110**, 261-266.

Hasemann, C. A., Kurumbail, R. G., Boddupalli, S. S., Peterson, J. A. & Deisenhofer, J. (1995). Structure and function of cytochromes *P*450: a comparative analysis of three crystal structures. *Structure,* **2**, 41-62.

Hiwatashi, A., Ichikawa, Y., Maruya, N., Yamano, T. & Aki, K. (1976). Properties of crystalline reduced nicotinamide adenine dinucleotide phosphate-adrenodoxin reductase from bovine adrenocortical mitochondria. *Biochemistry,* **15**, 3082-3090.

Holm, L. & Sander, C. (1993). Protein structure comparison by alignment of distance matrices. *J. Mol. Biol.* **233**, 123-138.

Ichikawa, Y. & Hiwatashi, A. (1982). The role of the sugar regions of components of the cytochrome *P*450-linked mixed-function oxidase (monooxygenase) system of bovine adrenocortical mitochondria. *Biochim. Biophys. Acta,* **705**, 82-91.

Ingelman, M., Bianchi, V. & Eklund, H. (1997). The three-dimensional structure of flavodoxin reductase from *Escherichia coli* at 1.7 Å resolution. *J. Mol. Biol.* **268**, 147-157.

Ishimura, K. & Fujita, H. (1997). Light and electron microscopic immunohistochemistry of the localization of adrenal steroidogenic enzymes. *Microsc. Res. Tech.* **36**, 445-453.

Jones, T. A., Zou, J.-Y., Cowan, S. W. & Kjeldgaard, M. (1991). Improved methods for building models in electron density maps and the location of errors in these models. *Acta Crystallog. sect. A,* **47**, 110-119.

Kabsch, W. (1988). Evaluation of single-crystal X-ray diffraction data from a position-sensitive detector. *J. Appl. Crystallog.* **21**, 916-924.

Karplus, P. A., Daniels, M. J. & Herriott, J. R. (1991). Atomic structure of ferredoxin-$NADP^+$ reductase: prototype for a structurally novel flavoenzyme family. *Science,* **251**, 60-66.

Kobayashi, K., Miura, S., Miki, M., Ichikawa, Y. & Tagawa, S. (1995). Interaction of NADPH-adrenodoxin reductase with $NADP^+$ as studied by pulse radiolysis. *Biochemistry,* **34**, 12932-12936.

Kuban, R.-J., Marg, A., Resch, M. & Ruckpaul, K. (1993). Crystallization of bovine adrenodoxin reductase in a new unit cell and its crystallographic characterization. *J. Mol. Biol.* **234**, 245-248.

Lambeth, J. D., Seybert, D. W. & Kamin, H. (1979). Ionic effects on adrenal steroidogenic electron transport. *J. Biol. Chem.* **254**, 7255-7264.

Lambeth, J. D., Seybert, D. W., Lancaster, J. R., Jr, Salerno, J. C. & Kamin, H. (1982). Steroidogenic electron transport in adrenal cortex mitochondria. *Mol. Cell. Biochem.* **45**, 13-31.

Lapko, A., Müller, A., Heese, O., Ruckpaul, K. & Heinemann, U. (1997). Preparation and crystallization of a cross-linked complex of bovine adrenodoxin and adrenodoxin reductase. *Proteins: Struct. Funct. Genet.* **28**, 289-292.

Leslie, A. G. W. (1990). Molecular data processing. In *Crystallographic Computing 5* (Moras, D., Podgarny, A. D. & Thierry, J. C., eds), pp. 50-61, Oxford University Press, Oxford, UK.

Lu, G., Campbell, W. H., Schneider, G. & Lindqvist, Y. (1994). Crystal structure of the FAD-containing fragment of corn nitrate reductase at 2.5 Å resolution: relationship to other flavoprotein reductases. *Structure,* **2**, 809-821.

Massey, V. (1995). Introduction: flavoprotein structure and mechanism. *FASEB J.* **9**, 473-475.

Miura, S. & Ishikawa, Y. (1994). Interaction of NADPH-adrenoferredoxin reductase with $NADP^+$ and adrenoferredoxin. *J. Biol. Chem.* **269**, 8001-8006.

Müller, A., Müller, J. J., Muller, Y. A., Uhlmann, H., Bernhardt, R. & Heinemann, U. (1998). New aspects of electron transfer revealed by the crystal structure of truncated bovine adrenodoxin, Adx(4-108). *Structure,* **6**, 269-280.

Nicholls, A., Sharp, K. A. & Honig, B. (1991). Protein folding and association: insights from the interfacial and thermodynamic properties of hydrocarbons. *Proteins: Struct. Funct. Genet.* **11**, 281-296.

Nishida, H., Inaka, K., Yamanaka, M., Kaida, S., Kobayashi, K. & Miki, K. (1995). Crystal structure of NADH-cytochrome b_5 reductase from pig liver at 2.4 Å resolution. *Biochemistry,* **34**, 2763-2767.

Nonaka, Y., Aibara, S., Sugiyama, T., Yamano, T. & Morita, Y. (1985). A crystallographic investigation on NADPH-adrenodoxin oxidoreductase. *J. Biochem.* **98**, 257-260.

Omura, T., Sanders, E., Estabrook, R. W., Cooper, D. Y. & Rosenthal, O. (1966). Isolation from adrenal cortex of a nonheme iron protein and a flavoprotein functional as a reduced triphosphopyridine nucleotide-cytochrome P-450 reductase. *Archives Biochem. Biophys.* **117**, 660-673.

Pochapsky, T. C., Ye, X. M., Ratnaswamy, G. & Lyons, T. A. (1994). An NMR-derived model for the solution structure of oxidized putidaredoxin, a 2-Fe, 2-S ferredoxin from *Pseudomonas*. *Biochemistry,* **33**, 6424-6432.

Sagara, Y., Wada, A., Takata, Y., Waterman, M. R., Sekimizu, K. & Horiuchi, T. (1993). Direct expression of adrenodoxin reductase in *Escherichia coli* and the functional characterization. *Biol. Pharm. Bull.* **16**, 627-630.

Schulz, G. E. (1980). Gene duplication in glutathione reductase. *J. Mol. Biol.* **138**, 335-347.

Schulz, G. E. (1992). Binding of nucleotides by proteins. *Curr. Opin. Struct. Biol.* **2**, 61-67.

Schulz, G. E., Schirmer, R. H., Sachsenheimer, W. & Pai, E. F. (1978). The structure of the flavoenzyme glutathione reductase. *Nature,* **273**, 120-124.

Stehle, T., Ahmed, S. A., Claiborne, A. & Schulz, G. E. (1991). Structure of NADH peroxidase from *Streptococcus faecalis* 10C1 refined at 2.16 Å resolution. *J. Mol. Biol.* **221**, 1325-1344.

Suhara, K., Nakayama, K., Takikawa, O. & Katagiri, M. (1982). Two forms of adrenodoxin reductase from mitochondria of bovine adrenal cortex. *Eur. J. Biochem.* **125**, 659-664.

Uhlmann, H., Kraft, R. & Bernhardt, R. (1994). C-terminal region of adrenodoxin affects its structural integrity and determines differences in its electron transfer function to cytochrome P-450. *J. Biol. Chem.* **269**, 22557-22564.

Vickery, L. E. (1997). Molecular recognition and electron transfer in the mitochondrial steroid hydroxylase system. *Steroids,* **62**, 124-127.

Vonrhein, C., Schmidt, U., Ziegler, G. A., Schweiger, S., Hanukoglu, I. & Schulz, G. E. (1999). Chaperone-assisted expression of authentic bovine adrenodoxin reductase in *Escherichia coli*. *FEBS Letters,* **443**, 167-169.

Waksmann, G., Krishnan, T. S. R., Williams, C. H., Jr & Kuriyan, J. (1994). Crystal structure of *Escherichia coli* thioredoxin reductase refined at 2 Å resolution. *J. Mol. Biol.* **236**, 800-816.

Wang, M., Roberts, D. L., Paschke, R., Shea, T. M., Masters, B. S. S. & Kim, J.-J. P. (1997). Three-dimensional structure of NADPH-cytochrome *P*450 reductase: prototype for FMN- and FAD-containing enzymes. *Proc. Natl Acad. Sci. USA,* **94**, 8411-8416.

Wartburton, R. J. & Seybert, D. W. (1995). Structural and functional characterization of bovine adrenodoxin reductase by limited proteolysis. *Biochim. Biophys. Acta,* **1246**, 39-46.

Edited by D. C. Rees

(Received 18 February 1999; received in revised form 19 April 1999; accepted 20 April 1999)